



**Synthesis of a Peptide-Universal Nucleotide Antigen:  
Towards Next-Generation Antibodies to Detect  
Topoisomerase I-DNA Covalent Complexes**

|                               |  |
|-------------------------------|--|
| Journal:                      | <i>Organic &amp; Biomolecular Chemistry</i>  |
| Manuscript ID                 | OB-COM-10-2015-002049.R2   |
| Article Type:                 | Paper  |
| Date Submitted by the Author: | 30-Mar-2016  |
| Complete List of Authors:     | Perkins, Angela; University of Minnesota, Medicinal Chemistry<br>Peterson, Kevin; Mayo Clinic, Oncology Research<br>Beito, Thomas; Mayo Clinic, Monoclonal Antibody Core<br>Flatten, Karen; Mayo Clinic, Oncology Research<br>Kaufmann, Scott; Mayo Clinic, Oncology Research<br>Harki, Daniel; University of Minnesota, Medicinal Chemistry |
|                               |  |



Journal Name

ARTICLE

## Synthesis of a Peptide-Universal Nucleotide Antigen: Towards Next-Generation Antibodies to Detect Topoisomerase I-DNA Covalent Complexes

Received 00th January 20xx,  
Accepted 00th January 20xx

DOI: 10.1039/x0xx00000x

www.rsc.org/

Angela L. Perkins,<sup>a</sup> Kevin L. Peterson,<sup>b</sup> Thomas G. Beito,<sup>c</sup> Karen S. Flatten,<sup>b</sup> Scott H. Kaufmann<sup>b</sup> and Daniel A. Harki<sup>a\*</sup>

The topoisomerase (topo) I-DNA covalent complex represents an attractive target for developing diagnostic antibodies to measure responsiveness to drugs. We report a new antigen, peptide **2**, and four murine monoclonal antibodies raised against **2** that exhibit excellent specificity for recognition of **2** in comparison to structurally similar peptides by enzyme-linked immunosorbent assays. Although topo I-DNA complex detection was not achieved in cellular samples by these new antibodies, a new strategy for antigen design is reported.

### Introduction

DNA topoisomerases (topos), enzymes that are present in both prokaryotes and eukaryotes, have evolved to alleviate torsional strain that accumulates during DNA strand separation.<sup>1</sup> Human topo I is highly abundant (up to 10<sup>6</sup> copies/cell) and relaxes torsional strain for a variety of nuclear processes, including replication, transcription and viral integration.<sup>1-3</sup> During the course of its normal catalytic cycle, topo I catalyzes a transesterification reaction that results in the formation of a covalent bond between the active site tyrosine of the enzyme and a 3'-phosphate in the DNA backbone, with concomitant formation of a nick in the DNA backbone that allows rotation of DNA around the intact strand (Figure 1).<sup>1-3</sup> After the DNA is relaxed, the enzyme reverses the transesterification reaction, thereby resealing the DNA backbone. Members of a widely used class of anticancer drugs, the camptothecins, interfere with this catalytic cycle by intercalating into DNA at the active site of DNA-bound topo I, inhibiting the religation step and altering the equilibrium toward covalent topo I-DNA complexes.<sup>4,5</sup> Interactions of these covalent topo I-DNA complexes with advancing replication forks or transcription complexes then result in further DNA damage, yielding cell death.<sup>6</sup> Based on their ability to somewhat selectively induce cancer cell death, several camptothecins are important anticancer agents.<sup>7</sup> In particular, irinotecan is FDA-approved for colorectal cancer

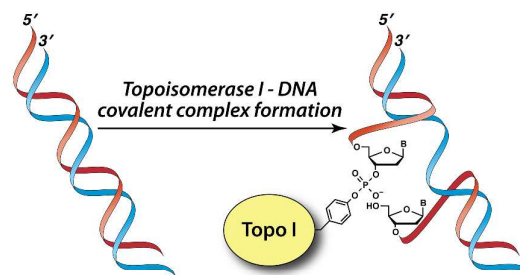


**Figure 1.** Formation of topoisomerase I-DNA covalent complex formation. B = nucleobase.

and is active against non-small cell lung, pancreatic, and breast cancers. Topotecan (TPT) is approved for ovarian, endometrial and small cell lung cancer therapy. Additional topo I poisons are under development.<sup>2, 7-10</sup>

The formation of covalent topo-DNA complexes is a critical first step in the cytotoxicity of molecules (termed poisons) that stabilize the covalent topo I-DNA complex. Cells with diminished or absent topo I form fewer covalent complexes and are resistant to this class of agents.<sup>11-14</sup> Conversely, alterations in the sequences of topo I enzymes that slow the religation step result in more covalent topo I-DNA complexes in the absence of drug and are lethal in model organisms.<sup>15</sup> These observations have provided the impetus for investigating the usefulness of topo I levels as predictive factors for response to the respective classes of agents.<sup>16</sup> Furthermore, given the potential of topo I poisons to cause severe toxicities in normal tissues, there is intense interest in predicting which patients are likely to respond (or not) to that class of molecules.

<sup>a</sup> Department of Medicinal Chemistry, University of Minnesota, 2231 6<sup>th</sup> Street SE, Minneapolis, MN 55455. E-mail: [daharki@umn.edu](mailto:daharki@umn.edu); Tel: 612-625-8687.

<sup>b</sup> Division of Oncology Research, Mayo Clinic, 200 First St., S.W., Rochester, MN 55905.

<sup>c</sup> Monoclonal Antibody Core, Mayo Clinic, 200 First St., S.W., Rochester, MN 55905. Electronic Supplementary Information (ESI) available: Supplemental Figures 1 & 2. See DOI: 10.1039/x0xx00000x

In view of the critical role of covalent topo-DNA complexes in the activity of these drugs, the measurement of covalent complexes represents an important step in developing these types of predictive assays. Topo-DNA complexes have been previously measured included alkaline elution,<sup>17-19</sup> *in vivo* complexing of enzyme (ICE) assays,<sup>20</sup> potassium-SDS precipitation assays,<sup>21-23</sup> neutral comet assays,<sup>24</sup> and rapid approach to DNA adduct recovery (RADAR) assays.<sup>25,26</sup> We have taken an immunological approach toward detecting the topo I-DNA covalent complex.

We recently reported the development of a novel monoclonal antibody, TopoIcc, that detects the topo-I DNA covalent complex, but not topo I alone or DNA, on immunoblots from camptothecin-treated cells and in immunofluorescence assays.<sup>27</sup> Unfortunately, the antibody was not suitable for assessing topo I-DNA covalent complexes by enzyme linked immunosorbant assay (ELISA),<sup>27</sup> a quantitative assay used for evaluating biological specimens from patients treated with anticancer drugs.<sup>28,29</sup> Therefore, we have begun the development of next-generation topo I-DNA covalent complex-targeting monoclonal antibodies using more complicated antigens designed to more closely mimic the covalent complex. Here, we report the preparation of a novel peptide antigen, **2**, which mimics the topo I active site and contains a universal nucleotide appended to the catalytic tyrosine (Figure 2). In addition, we report the development of four monoclonal antibodies against antigen **2** and their characterization.

## Results and Discussion

Antibody TopoIcc was raised against antigen **1**. We hypothesized that incorporation of a nucleotide onto the phosphorylated tyrosine may yield a superior antigen and result in antibodies that bind topo I-DNA covalent complexes more specifically. Our rationale was that additional structural complexity on the antigen through incorporation of a DNA fragment might yield a stronger epitope. We selected the incorporation of the known 'universal nucleoside', 1-ribofuranosyl-2'-deoxy-3-nitropyrrrole (3-NP),<sup>30,31</sup> to avoid

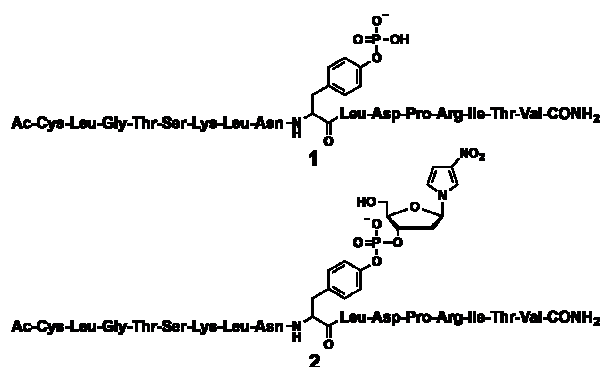
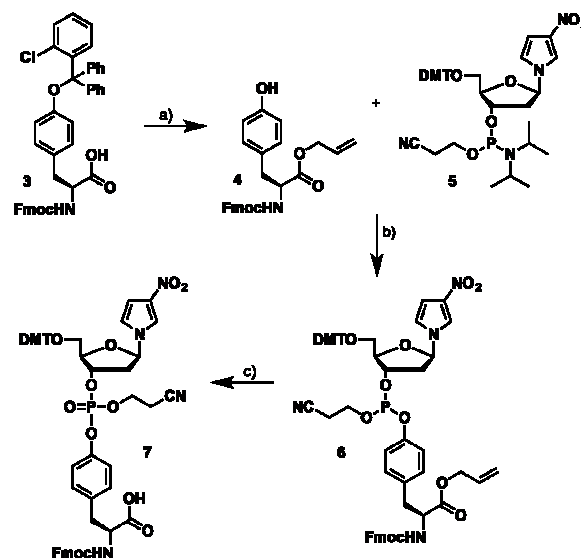


**Figure 2.** Antigen **1** and second-generation peptide-universal nucleotide antigen **2** used in this study.



**Scheme 1.** Synthesis of monomer for solid-phase peptide synthesis. Reagents and Conditions: a) i. allyl bromide, DIPEA, DMF; ii. CF<sub>3</sub>CO<sub>2</sub>H, CH<sub>2</sub>Cl<sub>2</sub>, 74% (2 steps); b) tetrazole, MeCN, CH<sub>2</sub>Cl<sub>2</sub>, 4 Å mol sieve, 69%; c) i. *t*-BuOOH, decane, CH<sub>2</sub>Cl<sub>2</sub>, 76%; ii. Pd(PPh<sub>3</sub>)<sub>4</sub>, PhSiH<sub>3</sub>, THF, 89%. sequence biases when detecting covalent complexes from patient samples. Consequently, we prepared target antigen **2**.

The coupling of sugars to amino acids or peptides through phosphate ester linkages, as well as the tethering of nucleosides (and –tides) to tyrosine and small peptides, has been established. The literature surrounding the majority of these couplings centers on the formation of the peptide linkage to the 5'-hydroxyl group of the nucleoside,<sup>32-36</sup> although linkage to the 3'-hydroxyl group has been established.<sup>37</sup> Our designed antigen, **2**, requires conjugation of the 3'-hydroxyl group of 3-NP to the catalytic tyrosine.

Our initial approach to the synthesis of **2** focused on conjugating 3-NP phosphoramidite **5** to the target tyrosine with the full 16-mer peptide bound to the solid-phase synthesis resin (rink amide resin; Figure S1). We synthesized the target peptide using standard solid-phase peptide synthesis (SPPS) techniques with the phenol of the target tyrosine protected with a 2-chlorotrityl group so that it could be selectively deprotected with CF<sub>3</sub>CO<sub>2</sub>H in CH<sub>2</sub>Cl<sub>2</sub> (2% acid), while keeping the remainder of the peptide fully protected and bound to resin. With the tyrosine side-chain deprotected, we reacted the on-resin peptide (Figure S1) with phosphoramidite **5** (tetrazole, MeCN, CH<sub>2</sub>Cl<sub>2</sub>, 4 Å MS), followed by conditions to oxidize the phosphite to phosphate (mCPBA), cleave the cyanoethyl group (20% piperidine in DMF), and cleave the peptide from resin (cleavage cocktail: 85:5:5:5 trifluoroacetic acid: distilled water: triisopropyl silane: ethane dithiol). Unfortunately, liquid chromatography-mass spectrometry (LC-MS) analysis of the crude material revealed no conjugation of phosphoramidite **5** and only the fully deprotected peptide was observed (**8**, Figure S2). A few different conditions for coupling and oxidation were screened, but an isolatable amount of antigen **2** was never obtained. We were unable to determine if the problem was

coupling of **5** to the resin-bound peptide or if the resulting phosphite (resulting from a productive coupling of **5**) was not oxidized to the phosphate since analysis of the peptide following resin cleavage conditions would not likely retain the phosphite linkage.

A second route was then developed for the preparation of **2**, where we adapted the method of Itzen and Hedberg that requires synthesis of the fully modified tyrosine amino acid followed by its utilization in SPPS.<sup>36,38,39</sup> This approach began with commercially available **3**, which was converted to the known, protected tyrosine **4** using a modification to the published procedure (Scheme 1).<sup>40</sup> Reaction of phenol **4** with commercially available phosphoramidite **5** in the presence of tetrazole yielded phosphite **6** in 69% yield. Oxidation of the phosphite to the phosphate was performed using conditions optimized for related compounds (*t*-BuOOH),<sup>36</sup> resulting in clean formation of the phosphate in 76% yield. Pd-catalyzed removal of the alloc protecting group provided target monomer **7** in 89% yield.<sup>41</sup>

With monomer **7** complete, antigen **2** was synthesized using standard Fmoc SPPS methodology. The peptide was built on rink amide resin using HBTU and *N*-methylmorpholine for amino acid couplings. The peptide was cleaved off resin using the cleavage cocktail described above. The crude peptide was then isolated via precipitation using cold ether (~3x amount of cleavage cocktail) and the white precipitate was collected via centrifugation. Purification of the resulting peptide by semi-preparative reverse-phase HPLC and mass spectrometry characterization confirmed the synthesis of **2** in 6% overall isolated yield and high purity (Figure 3).

Peptide **2** was then conjugated through its *N*-terminal cysteine to keyhole limpet hemocyanin and murine hybridomas that detect **2** were generated and cloned. Of 960 wells initially screened, four contained antibodies that differentially reacted with immunizing peptide **2** compared to non-modified topo I peptide **8** (Figure S2). Hybridomas were subcloned twice by limiting dilution to yield four monoclonal antibodies with strong preference for **2** (Figure 4A; 1D2, 4B11, 6F9, and 7E4). ELISA assays revealed the antibodies exhibited remarkable specificity for detection of nucleotide-peptide antigen **2** versus non-modified peptide **8**. Further analysis of 6F9 in comparison to previously reported TopoIcc<sup>27</sup> and RasGRP1<sup>42</sup> antibodies

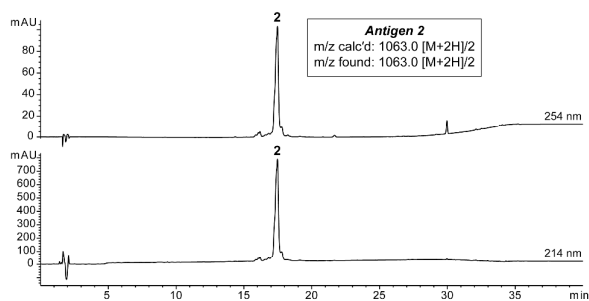


**Figure 3.** Analytical characterization of antigen **2** by analytical reverse-phase HPLC and mass spectrometry.

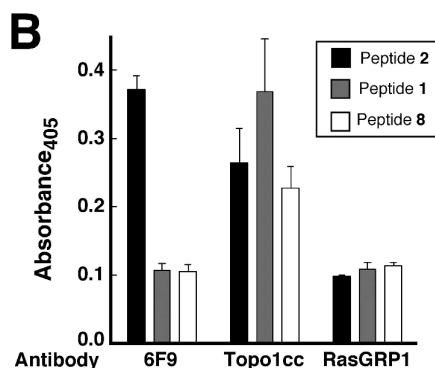
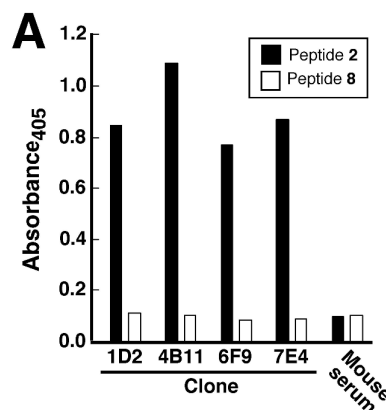


**Figure 4.** Characterization of antibodies by ELISA assays. (A) Concentrated cell culture supernatants from the indicated hybridomas and normal mouse serum were subjected to ELISA assays for their ability to detect **2** and the non-phosphorylated topo I peptide **8** (Figure S2). (B) Reactivity of 6F9 cell culture supernatant, TopoIcc (raised using antigen **1**), and RasGRP1 (unrelated control monoclonal antibody) against **2**, the phosphorylated topo I peptide **1** (Figure 2), and the non-phosphorylated topo I peptide **8** (Figure S2).

revealed that 6F9 was >3-fold selective for antigen **2** versus the phosphorylated topo I peptide **1** or non-phosphorylated topo I peptide **8**, whereas TopoIcc could not distinguish between these three peptides, although each were bound equivalently well (Figure 4B). RasGRP1, used as a negative control antibody, did not preferentially bind any of the three peptides examined. Unfortunately, none of the four antibodies generated using antigen **2** (1D2, 4B11, 6F9 or 7E4) was able to detect topo I-DNA covalent complexes from camptothecin-treated A549 cell lysates by immunoblotting (Figure 5A). In these analyses, A549 cells were treated with 5  $\mu$ M camptothecin or diluent, lysed, and subjected to CsCl<sub>2</sub> gradient sedimentation. Fractions containing protein (DNA-bound and free) were blotted onto nitrocellulose and probed with antibodies for total topo I, TopoIcc, or 6F9. TopoIcc selectively recognized DNA-bound topo I protein as previously reported,<sup>27</sup> whereas new antibody raised against **2**, 6F9, exhibited no binding. In subsequent immunofluorescence assays, A549 cells were treated with 1000 nM topotecan (30 mins), fixed, treated to render topo I-DNA complexes accessible, and then stained with TopoIcc or 6F9 antibody followed by fluorochrome-conjugated secondary

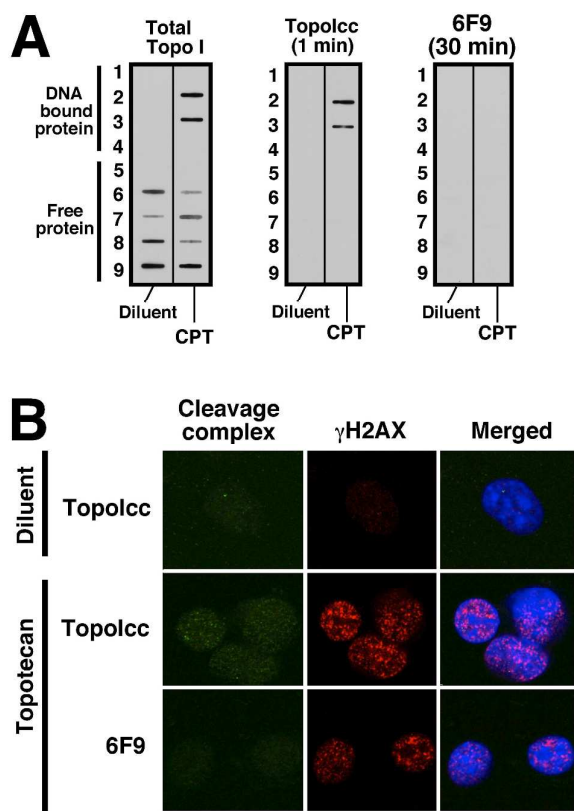


**Figure 5.** Comparison of antibodies for detection of topo I-DNA covalent complexes. (A) A549 lung cancer cells were treated with 5  $\mu\text{M}$  camptothecin (CPT) or diluent, lysed, then subjected to  $\text{CsCl}_2$  gradient sedimentation. Fractions containing DNA or free protein were blotted onto nitrocellulose and probed with the indicated antibodies. (B) Immunofluorescence assays for topo I-DNA covalent complexes *in situ*. A549 cells were dosed with 1000 nM topotecan for 30 min, fixed, treated with 1% SDS to render the topo I-DNA adduct accessible, and labelled with the indicated monoclonal antibody followed by Alexa Fluor 488-labeled anti-mouse IgG (green). Simultaneous staining with rabbit anti-phospho-Ser<sup>139</sup>-Histone H2AX and Alexa Fluor 568-labeled anti-rabbit IgG (red) as well as the DNA binding dye Hoechst 33258 (blue) permitted visualization of nuclei with TPT-induced DNA damage, which is a downstream consequence of successful stabilization of topo I-DNA covalent complexes.

antibody. These assays revealed topo I-DNA covalent complex formation in TPT-treated cells stained with TopoIcc (as reported previously),<sup>27</sup> but not with 6F9, which further corroborates our immunoblot data (Figure 5B). Antibodies 1D2, 4B11 and 7E4 similarly failed to detect covalent topo I-DNA complexes in cell lysates and in fixed cells. Based on these results, we hypothesize that the 3-NP nucleobase was too dominant of an antigen and, therefore, 6F9 and related antibodies raised against **2** are selective for nucleotides bearing only 3-nitropyrrole nucleobases.

## Conclusions

Although antibodies raised against antigen **2** failed to detect the covalent topo I-DNA complex from cancer cell lysates or fixed cells, our studies demonstrate the utility of peptide-nucleotide conjugates as antigens and reinforce the strong immunogenicity of nitroaromatic compounds. Incorporation of additional structural complexity on the catalytic tyrosine clearly contributed to the antigenicity of the peptide. Unfortunately, our data suggest this modification was overly dominant and yielded antibodies with apparent specificity for nucleotides bearing only the 3-nitropyrrole nucleobase. Other antigens are currently under investigation in our laboratories and those results, along with the performance of antibodies raised against these third-generation antigens, will be reported in due course.

## Experimental Section.

### Monomer Synthesis.

**General synthesis information.** Chemical reagents were purchased from commercial sources and used without additional purification unless explicitly noted. Fmoc protected amino acids and peptide synthesis resins were from EMD Biosciences. 1-Ribofuranosyl-2'-deoxy-3-nitropyrrole (3-NP) phosphoramidite **5** was purchased from Glen Research. Bulk solvents were from Fisher Scientific. Anhydrous solvents were obtained from an MBraun solvent purification system. Reaction were performed under an atmosphere of dry  $\text{N}_2$  where noted. Silica gel chromatography was performed on a Teledyne-Isco Combiflash Rf-200 instrument using Rediseq Rf Gold High Performance silica gel columns (Teledyne-Isco). Analytical HPLC analysis was performed on an Agilent 1200 series instrument equipped with a diode array detector and a Zorbax SB-C18 column (4.6 x 150 mm, 3.5  $\mu\text{m}$ , Agilent Technologies). Nuclear magnetic resonance (NMR) spectroscopy using a Bruker Avance instrument operating at 400 MHz (for  $^1\text{H}$ ), 125 MHz (for  $^{13}\text{C}$ ), or 161 MHz (for  $^{31}\text{P}$ ) at ambient temperature. Chemical shifts are reported in parts per million and normalized to internal solvent peaks or tetramethylsilane ( $\delta = 0$  ppm). Mass spectrometry was recorded in positive-ion mode on a Bruker BioTOF II instrument.

**Synthesis of phosphite 6.** Protected tyrosine **4** was synthesized as previously described<sup>40</sup> with the exception that starting material **3** (commercially available) contained a 2-chlorotrityl protecting group on the phenol. After introduction of the Alloc protecting group as previously reported,<sup>40</sup> the 2-chlorotrityl protecting group was cleaved with  $\text{CF}_3\text{CO}_2\text{H}$  in  $\text{CH}_2\text{Cl}_2$  (2%). Spectral data for **4** was identical to that previously reported.<sup>40</sup> Next, **4** (149 mg, 0.343 mmol), phosphoramidite **5** (251 mg, 0.343 mmol), and one molecular sieve (4 $\text{\AA}$ , oven dried) was placed in anhydrous  $\text{CH}_2\text{Cl}_2$  (1.7 mL) under  $\text{N}_2$  and cooled to 0 $^\circ\text{C}$ . A solution of tetrazole in  $\text{CH}_3\text{CN}$  (0.47 M, 1.5 mL) was added. This solution was slowly warmed to room temperature. After 18 hours, the reaction solution was poured into additional  $\text{CH}_2\text{Cl}_2$  (30 mL) and washed with brine (2 x 30 mL). The organic layer was then dried over  $\text{Na}_2\text{SO}_4$ , filtered and concentrated *in vacuo*. The resulting oil was purified via silica

gel chromatography using 25% EtOAc in hexanes to give 255 mg (69%) of phosphite **6** (two diastereomers) as a colorless foam.  $^1\text{H}$  NMR ( $\text{CDCl}_3$ ):  $\delta$  7.76 (d,  $J = 7.8$  Hz, 2H), 7.67 (d,  $J = 2.1$  Hz, 1H), 7.59 (d,  $J = 7.7$  Hz, 2H), 7.45 – 7.33 (m, 4H), 7.33 – 7.14 (m, 10H), 7.03 (d,  $J = 7.8$  Hz, 2H), 6.93 – 6.83 (m, 2H), 6.85 – 6.75 (m, 4H), 6.78 – 6.70 (m, 2H), 5.94 – 5.81 (m, 2H), 5.38 – 5.22 (m, 2H), 5.10 – 5.04 (m, 1H), 4.74 – 4.58 (m, 3H), 4.43 (dd,  $J = 10.7, 7.2$  Hz, 1H), 4.35 (dt,  $J = 10.9, 5.3$  Hz, 1H), 4.30 (m, 1H), 4.18 (t,  $J = 6.9$  Hz, 1H), 4.13 – 3.94 (m, 2H), 3.80 (s, 3H), 3.77 (s, 1H), 3.33 (dd,  $J = 7.2, 4.1$  Hz, 2H), 3.20 – 3.00 (m, 2H), 2.61 (t,  $J = 6.2$  Hz, 1H), 2.58 – 2.39 (m, 3H);  $^{31}\text{P}$  NMR ( $\text{CDCl}_3$ ):  $\delta$  133.59, 132.98.

**Monomer 7.** A solution of phosphite **6** (255 mg, 0.238 mmol) in anhydrous  $\text{CH}_2\text{Cl}_2$  (2.4 mL) was cooled to  $0^\circ\text{C}$ . A solution of *t*-butylhydroperoxide (5–6 M in decane, 65  $\mu\text{L}$ ) was slowly added. The solution was slowly warmed to room temperature. After 2 hours, the resulting solution was concentrated to a colorless foam, which was purified on silica gel using an increasing gradient of 15 – 25% EtOAc in hexanes to yield the phosphate (196 mg, 76%) as a colorless foam.  $^1\text{H}$  NMR ( $\text{CDCl}_3$ ):  $\delta$  7.76 (d,  $J = 7.6$  Hz, 2H), 7.65 (dt,  $J = 7.2, 2.1$  Hz, 1H), 7.56 (d,  $J = 7.4$  Hz, 2H), 7.44 – 7.33 (m, 4H), 7.33 – 7.17 (m, 10H), 7.08 (d,  $J = 8.2$  Hz, 4H), 7.08 (d,  $J = 8.2$  Hz, 4H), 6.85 – 6.77 (m, 4H), 6.75 – 6.59 (m, 2H), 5.98 – 5.78 (m, 2H), 5.39 – 5.23 (m, 3H), 5.19 (app q,  $J = 5.7$  Hz, 1H), 4.74 – 4.50 (m, 2H), 4.47 – 4.16 (m, 5H), 3.78 (s, 3H), 3.77 (s, 3H), 3.41 – 3.28 (m, 2H), 3.22 – 3.00 (m, 2H), 2.78 – 2.44 (m, 4H);  $^{13}\text{C}$  NMR ( $\text{CDCl}_3$ ):  $\delta$  171.2, 158.7, 155.6, 149.0, 144.1, 143.8, 143.7, 141.3, 137.6, 137.5, 135.2, 133.8, 131.2, 131.0, 130.0, 128.0, 127.8, 127.7, 127.0, 125.0, 120.0, 119.7, 119.6, 119.5, 119.2, 113.3, 106.1, 88.6, 87.1, 86.9, 85.6, 71.7, 66.9, 66.3, 60.4, 55.2, 54.8, 47.2, 40.6, 37.6, 19.8.  $^{31}\text{P}$  NMR ( $\text{CDCl}_3$ ):  $\delta$  -7.73. MS-ESI $^+$   $m/z$  [ $\text{M} + \text{H}$ ] calculated for  $\text{C}_{60}\text{H}_{58}\text{N}_4\text{O}_{14}\text{P}$ , 1089.4; found 1089.5.

A solution of the resulting phosphate (180 mg, 0.165 mmol) in anhydrous THF (3.3 mL) was degassed and flushed with  $\text{N}_2$  at room temperature.  $\text{Pd}(\text{PPh}_3)_4$  (10 mg, 0.008 mmol) was then added followed by  $\text{PhSiH}_3$  (30  $\mu\text{L}$ , 0.24 mmol). The reaction mixture was stirred at room temperature under  $\text{N}_2$  for 5 hours. The reaction mixture was then poured into distilled  $\text{H}_2\text{O}$  (20 mL) and extracted with EtOAc (2 x 15 mL). The organic layer was dried over  $\text{Na}_2\text{SO}_4$ , filtered and concentrated *in vacuo*. The resulting foam was purified via silica gel chromatography using 1% MeOH in  $\text{CH}_2\text{Cl}_2$  to obtain 154 mg (89%) of monomer **7** as a colorless foam.  $^1\text{H}$  NMR ( $\text{CDCl}_3$ ):  $\delta$  7.75 (d,  $J = 7.5$  Hz, 2H), 7.64 (s, 1H), 7.56 (d,  $J = 7.5$  Hz, 2H), 7.42 – 7.33 (m, 4H), 7.33 – 7.16 (m, 10H), 7.16 – 6.99 (m, 4H), 6.85 – 6.77 (m, 4H), 6.73 – 6.65 (m, 2H), 5.95 – 5.77 (m, 1H), 5.49 (d,  $J = 7.5$  Hz, 1H), 5.24 – 5.14 (m, 1H), 4.70 – 4.58 (m, 1H), 4.44 (dd,  $J = 10.6, 6.9$  Hz, 1H), 4.37 – 4.13 (m, 4H), 3.76 (s, 6H), 3.39 – 3.28 (m, 2H), 3.27 – 3.07 (m, 2H), 2.78 – 2.42 (m, 4H);  $^{31}\text{P}$  NMR ( $\text{CDCl}_3$ ):  $\delta$  -7.88. MS-ESI $^+$   $m/z$  [ $\text{M} + \text{H}$ ] calculated for  $\text{C}_{57}\text{H}_{54}\text{N}_4\text{O}_{14}\text{P}$ , 1049.3; found 1049.3.

#### Solid-Phase Peptide Synthesis (SPPS).

**General information.** Automated SPPS was performed using a Protein Technologies PS3 peptide synthesizer. Peptide synthesizer grade DMF was purchased from Fisher Scientific and used for all manual and automated couplings, washes and deprotections.  $\text{N}_2$  was used to aid in the transfer of reagents into the SPPS vessel and for agitation of resin during synthesis. Rink Amide MBHA low-loading resin (0.38 mmol/g) was used. The resin was swelled with DMF (2 x 15 mins) before use. *N*-terminal Fmoc cleavage was performed by using a solution of 20% piperidine in DMF (2 x 5 mins), following by washing with DMF (6 x 0.5 mins). Fmoc-protected amino acids (4 eq) and *O*-benzotriazole-1-yl-*N,N,N,N*-tetramethyluronium hexafluorophosphate (HBTU, 4 eq) were dissolved in a 0.4 M solution of *N*-methylmorpholine (NMM) in DMF to form the activated ester. This solution was added to the resin and agitated for 20 minutes to couple. The solution was then drained from the resin bound peptide and resin was rinsed with DMF (3 x 0.5 mins). The cycle of deprotection, washing, coupling with Fmoc-protected amino acids, and final washing was repeated for each of the automated couplings of amino acids.

**Synthesis of Peptide 2.** After coupling the first 7 amino acids, the *N*-terminal Fmoc group was cleaved followed by subsequent washings. The free amino *N*-terminal peptide on resin was then transferred to a manual SPPS vessel. To the SPPS vessel was added a solution of **7** (3 eq), HBTU (3 eq), and 2,6-lutidine (8 eq) in DMF (4 mL). This coupling mixture was then gently shaken with the resin-bound peptide using a wrist-action shaker. After 24 hours, the solution was drained and resin was rinsed with DMF (4 mL) with gentle shaking (3 x 5 mins). A small sample of resin was removed, cleaved with a solution of 95:2.5:2.5 trifluoroacetic acid: distilled water: triisopropyl silane, concentrated and the crude sample was analyzed by LC-MS to verify coupling. MS-ESI $^+$   $m/z$  [ $\text{M} + \text{H}$ ] calculated for  $\text{C}_{72}\text{H}_{99}\text{N}_{15}\text{O}_{21}\text{P}$ , 1540.7; found 1540.9.

The resin-bound peptide was then returned to an automated SPPS vessel. The automated synthesis recommenced with deprotection of the *N*-terminal Fmoc group of incorporated monomer **7**. Automated synthesis was performed as previously described to install the additional 8 amino acids. After final deprotection, acetic anhydride (2 mL) was dissolved in 0.4M NMM in DMF and reacted with the resin-bound peptide for 20 mins to acylate the *N*-terminal amine. The protected, resin-bound peptide was then washed with DMF (3 x 0.5 mins).

The peptide was transferred back to a manual SPPS vessel and was deprotected and cleaved from resin using a solution (10 mL) of trifluoroacetic acid: distilled water: triisopropyl silane: ethane dithiol (85:5:5:5). The mixture was agitated for 30 minutes, followed by draining of the peptide cleavage solution into a 50 mL centrifuge tube. The peptide was precipitated by the addition of cold diethyl ether (~30 mL). The white precipitate was isolated by centrifugation (4000 rpm, 5 min,  $25^\circ\text{C}$ ). The crude peptide was purified via semi-preparative HPLC chromatography using distilled and deionized  $\text{H}_2\text{O}$  (with 0.1% TFA) and an increasing gradient of MeCN (with 0.1% TFA) on a Zorbax SB-C18 column (21.2 x

250 mm, 7  $\mu$ m, Agilent Technologies). After purification, the peptide was analyzed by analytical HPLC (Figure 3) and mass spectrometry. MS-ESI<sup>+</sup>  $m/z$  [M+2H]<sup>2+</sup> calculated for C<sub>90</sub>H<sub>150</sub>N<sub>24</sub>O<sub>31</sub>PS, 1063.0; found 1063.0.

#### Monoclonal Antibody Generation.

Peptide **2** was conjugated through its *N*-terminal cysteine to keyhole limpet hemocyanin as an antigen and murine hybridomas that detect **2** were generated and cloned as described by de St. Groth and Scheidegger.<sup>43</sup> Primary screening of culture supernatants was performed by ELISA.

#### ELISA for Antibody Specificity.

Immobilon II ELISA plates (Thermo) were coated with 1  $\mu$ g/well of the indicated peptide in 100 mM sodium carbonate buffer overnight at 4 °C, washed with calcium- and magnesium-free Dulbecco's phosphate buffered saline (PBS), and blocked with 3% bovine serum albumin in PBS. Wells were incubated with concentrated culture supernatant from cloned hybridoma lines for 1.5-2 h, washed three times with PBS containing 0.05% Tween 20, incubated for alkaline phosphatase-conjugated goat anti-mouse IgG (Sigma-Aldrich) at 0.2  $\mu$ g/mL for 1 h, washed four times with PBS containing 0.05% Tween 20, incubated for 5 min in 10 mM diethanolamine (pH 9.5) and then reacted with 1 mg/mL *p*-nitrophenyl phosphate in 10 mM diethanolamine for 12 min before absorbance was read at 405 nm.

#### ICE Assays.

ICE assays were performed as described.<sup>44</sup> Briefly, A549 cells (40-60% confluent) in 100 mm tissue culture plates were incubated for 60 min at 37 °C with DMSO or 5  $\mu$ M camptothecin in serum-free RPMI 1640 medium containing 10 mM HEPES, pH 7.4. After treatment, cells were rapidly lysed in 1 mL lysis buffer [10 mM Tris-HCl, pH 8.0, containing 1% sodium lauroyl sarcosinate (Sigma-Aldrich) and 1 mM EDTA]. The lysates were layered on a 6 mL CsCl<sub>2</sub> gradient and sedimented at 125,000  $\times$  g for 21 h at 20 °C. Fractions (0.5 mL each) were collected from the bottom of each gradient and slot-blotted onto nitrocellulose membranes, which were incubated for 2 h in TSM buffer consisting of 10% (w/v) powdered milk, 150 mM NaCl, 10 mM Tris-HCl (pH 7.4) and 1 mM sodium azide. Blots were then incubated overnight at 4 °C with C-21 anti-topo I IgM antibody (a kind gift of Y.-C. Cheng, Yale University; New Haven, CT), TopoIcc,<sup>24</sup> or monoclonal 6F9 followed by secondary antibodies and enhanced chemiluminescence detection reagents as previously described.<sup>45</sup>

#### Immunofluorescence Analysis.

A549 cells grown in RPMI 1640 medium with 10% heat-inactivated fetal calf serum, 100 U/mL penicillin G, 100  $\mu$ g/mL streptomycin and 2 mM glutamine on ethanol sterilized coverslips were treated for 30 min with 1000 nM topotecan or diluent (0.1% DMSO), fixed for 15 min at 4 °C in 4% (w/v) paraformaldehyde in calcium- and magnesium-free Dulbecco's phosphate buffered saline (PBS), and permeabilized with

0.25% (v/v) Triton X-100 in PBS for 15 min at 4 °C. To render the DNA-protein crosslinks more accessible to antibody, the coverslips were incubated in 1% (w/v) SDS in PBS at 20-22 °C for 5 min, washed five times with wash buffer [0.1% (w/v) bovine serum albumin and 0.1% (w/v) Triton X-100 in PBS], and blocked in TSM buffer. Coverslips were incubated overnight at 4 °C in murine anti-topoisomerase I-DNA covalent complex antibody (6F9 or TopoIcc) and rabbit anti-phospho-Ser<sup>139</sup>-H2AX (Millipore, Billerica, MA, used to mark damaged DNA) diluted in PBS containing 5% (v/v) goat serum, washed extensively with wash buffer over 20 min, and stained with Alexa Fluor 488-conjugated anti-mouse IgG and Alex Fluor 568-conjugated anti-rabbit IgG (Invitrogen) diluted 1:1000 in PBS/5% goat serum for 1 h in subdued light; washed 5-6 times with wash buffer over 20 min; stained with 1  $\mu$ g/mL Hoechst 33258 in PBS; and mounted using ProLong antifade reagent (Invitrogen; Carlsbad, CA). Images were captured on a LSM 710 scanning confocal microscope (Carl Zeiss AG; Oberkochen, Germany) using a 63X/1.2 W Korr C-Apo objective and processed using Zeiss Zen software and Adobe Photoshop CS3.

#### Acknowledgements

This work was supported by a grant from the Minnesota Partnership for Biotechnology and Medical Genomics (#10.03 to DAH & SHK). Mass spectrometry was performed at the Analytical Biochemistry Core Facility of the University of Minnesota Masonic Cancer Center, which is supported by the NIH (P30-CA77598).

#### Notes and references

1. J. C. Wang, *Nat Rev Mol Cell Biol*, 2002, **3**, 430-440.
2. Y. Pommier, *Nat Rev Cancer*, 2006, **6**, 789-802.
3. J. J. Champoux, *Annu Rev Biochem*, 2001, **70**, 369-413.
4. B. L. Staker, M. D. Feese, M. Cushman, Y. Pommier, D. Zembower, L. Stewart and A. B. Burgin, *J Med Chem*, 2005, **48**, 2336-2345.
5. B. L. Staker, K. Hjerrild, M. D. Feese, C. A. Behnke, A. B. Burgin and L. Stewart, *Proc Natl Acad Sci USA*, 2002, **99**, 15387-15392.
6. T. K. Li and L. F. Liu, *Annu Rev Pharmacol Toxicol*, 2001, **41**, 53-77.
7. Y. Pommier, *ACS Chem Biol*, 2013, **8**, 82-95.
8. B. N. Mow and S. H. Kaufmann, in *Camptothecins in Cancer Therapy*, eds. V. R. Adams and T. G. Burke, Humana Press, Totowa, NJ, 2005, pp. 421-450.
9. L. Chazin Ede, R. Reis Rda, W. T. Junior, L. F. Moor and T. R. Vasconcelos, *Mini Rev Med Chem*, 2014, **14**, 953-962.
10. C. Alemany, *Curr Oncol Rep*, 2014, **16**, 367.
11. W. K. Eng, L. Faucette, R. K. Johnson and R. Sternglanz, *Mol Pharmacol*, 1988, **34**, 755-760.
12. J. Nitiss and J. C. Wang, *Proc Natl Acad Sci U S A*, 1988, **85**, 7501-7505.
13. W. K. Eng, F. L. McCabe, K. B. Tan, M. R. Mattern, G. A. Hofmann, R. D. Woessner, R. P. Hertzberg and R. K. Johnson, *Mol Pharmacol*, 1990, **38**, 471-480.

14. M. A. Bjornsti, P. Benedetti, G. A. Viglianti and J. C. Wang, *Cancer Res*, 1989, **49**, 6318-6323.
15. P. Fiorani, J. F. Amatruda, A. Silvestri, R. H. Butler, M. A. Bjornsti and P. Benedetti, *Mol Pharmacol*, 1999, **56**, 1105-1115.
16. M. S. Braun, S. D. Richman, P. Quirke, C. Daly, J. W. Adlard, F. Elliott, J. H. Barrett, P. Selby, A. M. Meade, R. J. Stephens, M. K. Parmar and M. T. Seymour, *J Clin Oncol*, 2008, **26**, 2690-2698.
17. M. R. Mattern, S. M. Mong, H. F. Bartus, C. K. Mirabelli, S. T. Crooke and R. K. Johnson, *Cancer Res*, 1987, **47**, 1793-1798.
18. Y. H. Hsiang, L. F. Liu, M. E. Wall, M. C. Wani, A. W. Nicholas, G. Manikumar, S. Kirschenbaum, R. Silber and M. Potmesil, *Cancer Res*, 1989, **49**, 4385-4389.
19. K. W. Kohn, *Bioessays*, 1996, **18**, 505-513.
20. D. Subramanian, C. S. Furbee and M. T. Muller, in *DNA Topoisomerase Protocols: Volume II: Enzymology and Drugs*, eds. M.-A. Bjornsti and N. Osheroff, Humana Press, Totowa, NJ, 2001, pp. 137-147.
21. C. J. Li, L. Averboukh and A. B. Pardee, *J Biol Chem*, 1993, **268**, 22463-22468.
22. L. F. Liu, T. C. Rowe, L. Yang, K. M. Tewey and G. L. Chen, *J Biol Chem*, 1983, **258**, 15365-15370.
23. M. T. Muller, C. S. Bolles and D. S. Parris, *J Gen Virol*, 1985, **66**, 1565-1574.
24. A. Zhang, Y. L. Lyu, C. P. Lin, N. Zhou, A. M. Azarova, L. M. Wood and L. F. Liu, *J Biol Chem*, 2006, **281**, 35997-36003.
25. K. Kiianitsa and N. Maizels, *Nucleic Acids Res*, 2013, **41**.
26. K. Kiianitsa and N. Maizels, *Nucleic Acids Res*, 2014, **42**.
27. A. G. Patel, K. S. Flatten, K. L. Peterson, T. G. Beito, P. A. Schneider, A. L. Perkins, D. A. Harki and S. H. Kaufmann, *Nucleic Acids Res*, doi:10.1093/nar/gkw109.
28. S. Kummar, R. Kinders, M. E. Gutierrez, L. Rubinstein, R. E. Parchment, L. R. Phillips, J. Ji, A. Monks, J. A. Low, A. Chen, A. J. Murgo, J. Collins, S. M. Steinberg, H. Eliopoulos, V. L. Giranda, G. Gordon, L. Helman, R. Wiltrout, J. E. Tomaszewski and J. H. Doroshow, *J Clin Oncol*, 2009, **27**, 2705-2711.
29. T. D. Pfister, M. Hollingshead, R. J. Kinders, Y. Zhang, Y. A. Evrard, J. Ji, S. A. Khin, S. Borgel, H. Stotler, J. Carter, R. Divelbiss, S. Kummar, Y. Pommier, R. E. Parchment, J. E. Tomaszewski and J. H. Doroshow, *PLoS One*, 2012, **7**.
30. D. Loakes, *Nucleic Acids Res*, 2001, **29**, 2437-2447.
31. R. Nichols, P. C. Andrews, P. Zhang and D. E. Bergstrom, *Nature*, 1994, **369**, 492-493.
32. L. Debethune, G. Kohlhagen, A. Grandas and Y. Pommier, *Nucleic Acids Res*, 2002, **30**, 1198-1204.
33. L. Debethune, V. Marchan, G. Fabregas, E. Pedroso and A. Grandas, *Tetrahedron*, 2002, **58**, 6965-6978.
34. N. Kriek, D. V. Filippov, H. van den Elst, N. J. Meeuwenoord, G. I. Tesser, J. H. van Boom and G. A. van der Marel, *Tetrahedron*, 2003, **59**, 1589-1597.
35. P. Li and B. R. Shaw, *Org Lett*, 2002, **4**, 2009-2012.
36. C. Smit, J. Blumer, M. F. Eerland, M. F. Albers, M. P. Muller, R. S. Goody, A. Itzen and C. Hedberg, *Angew Chem Int Ed Engl*, 2011, **50**, 9200-9204.
37. A. C. Raymond, B. L. Staker and A. B. Burgin, *J. Biol. Chem.*, 2005, **280**, 22029-22035.
38. C. Hedberg and A. Itzen, *ACS Chem Biol*, 2015, **10**, 12-21.
39. M. P. Muller, M. F. Albers, A. Itzen and C. Hedberg, *ChemBioChem*, 2014, **15**, 19-26.
40. S. Ficht, R. J. Payne, R. T. Guy and C. H. Wong, *Chem Eur J*, 2008, **14**, 3620-3629.
41. M. Dessolin, M. G. Guillerez, N. Thieriet, F. Guibe and A. Loffet, *Tetrahedron Lett*, 1995, **36**, 5741-5744.
42. H. Ding, J. Hackbarth, P. A. Schneider, K. L. Peterson, X. W. Meng, H. Dai, T. E. Witzig and S. H. Kaufmann, *Blood*, 2011, **118**, 4872-4881.
43. S. F. de St. Groth and D. Scheidegger, *J Immunol Meth*, 1980, **35**, 1-21.
44. D. Subramanian, C. S. Furbee and M. T. Muller, *Methods in molecular biology (Clifton, N.J.)*, 2001, **95**, 137-147.
45. S. H. Kaufmann, *Anal Biochem*, 2001, **296**, 283-286.